

Preparation and Characterization of Barium Hexaferrite thin films

Dissertation submitted in fulfillment of the requirements for the Degree of

MASTER OF SCIENCE

By

JATINDER SINGH
(301504017)



Under the supervision of

Dr. PUNEET SHARMA

School of Physics & Material science

THAPAR INSTITUTE OF ENGINEERING AND TECHNOLOGY

PATIALA (147001)

PUNJAB

DEDICATED
TO
MY FAMILY

CERTIFICATE


I hereby certify that the work which is being presented in this report entitled, "Preparation and characterization of Barium hexaferrite thin films" as a part of curriculum during Master of Science in Physics, submitted to School of Physics & Material Science of Thapar University, Patiala, is an authentic record of my own work carried under the supervision of Dr. Puneet Sharma, SPMS. It refers others researcher's work which are duly listed in the reference section. The matter contained in this report has not been submitted, neither in part or in full to any other degree to any other university or institute except as reported in text and references.

Place: Patiala
Date: 17th July, 2017


(Jatinder Singh)
Roll No: 301504017

This is to certify that the above mentioned statement of the student is correct to the best of my knowledge and belief.

Date: 17th July, 2017


Dr. Puneet Sharma
Associate Professor
School of Physics & Material Science
Thapar University, Patiala

ACKNOWLEDGEMENT

I would like to thank **Dr. Puneet Sharma**, Associate Professor (SPMS), for giving me a chance to work under his supervision, without whose help and constant guidance this thesis would have not taken shape. I am extremely thankful to **Dr. O. P. Pandey**, Dean of Research, for their co-operation and encouragement. I am also thankful to all staff members of SPMS, for their constant cooperation in experimental work.

I am highly thankful to my senior PhD scholar Santhosh Kumar Mahadevan, Chhavi Pahwa, Shivani Jindal, and Anoop Partap Singh who provided their valuable guidance and suggestions during the course of the work. I acknowledge and thank my elders and my relatives for their support and motivation. I am very thankful to my parents for their constant cooperation, inspiration, patience, blessing and moral support.

I can never forget to acknowledge the funding agency DST (SERB/F/2947/2014-2015) for providing me financial support.

A handwritten signature in black ink, consisting of a stylized 'S' followed by 'P' and 'D', with a horizontal line underneath.

Table of content:

Abstract.....8

Chapter 1 Introduction.....9

1.1 Classification of hexaferrites.....10

1.2 Introduction of M-type hexaferrite.....10

1.3 Structure and properties.....10

1.4 Synthesizing techniques for hexagonal ferrites.....11

 1.4.1 Solid State Synthesis Method.....11

1.5 Thin films deposition techniques.....12

1.6 Physical vapour deposition.....13

 1.6.1 Pulse laser deposition.....13

 1.6.2 Thermal evaporation.....14

 1.6.3 Sputtering15

Chapter 2 Literature review.....17

Chapter 3 Experimental details.....26

3.1 Preparation of BaM powder.....26

3.2 Target preparation.....27

3.3 Thin film preparation.....30

3.4 Characterization techniques.....30

Chapter 4 Results and discussion.....32

4.1 Characterization of BaM powder.....32

4.2 Characterization of BaM thin films.....34

 4.2.1 Effect of deposition time.....34

 4.2.1 Effect of annealing temperature.....36

Conclusion39

References.....40

List of figures:

Figure 1.1 Phase diagram.....9

Figure 1.1 Magnetoplumbite structure.....11

Figure 1.2 Pulse laser deposition.....14

Figure 1.3 Thermal evaporation.....15

Figure 1.4 Sputtering.....16

Figure 3.1 Ball mill.....26

Figure 3.2 Vibratory mill.....27

Figure 3.3 Furnace.....27

Figure 3.4 Pressing of BaM powder.....28

Figure 3.5 BaM Target.....28

Figure 3.6 Magnetron Sputtering unit.....30

Figure 4.5 XRD pattern of pure BaM powder.....32

Figure 4.6 (a-b) SEM micrograph and EDS analysis image of pure BaM powder.....33

Figure 4.3 *M-H* loop of pure BaM powder.....33

Figure 4.4 XRD patterns of BaM thin films for different deposition time.....34

Figure 4.5 *M-H* loops of (parallel and perpendicular) BaM thin films deposited
for (a) 15 min (b) 30 min (c) 45 min (d) 60 min annealed at 1000°C.....35

Figure 4.6 XRD patterns of BaM thin films for different annealing temperatures.....36

Figure 4.7 Hysteresis loops of (in-plane and out-plane) 1 hour sputtered BaM
thin films annealed at (a) 700°C (b) 800°C (c) 900°C (d) 1000°C.....37

Figure 4.8 Surface morphology of BaM thin films deposited for
(a) 45 min (b) 60 min annealed at 1000°C38.

List of flow chart:

Flowchart 1 Thin film deposition techniques.....12
Flowchart 2: Preparation of BaM Target29

List of tables:

Table 1 Literature review summary.....22
Table 2 Variation in H_c , M_r , M_s and Sq of BaM thin films for different
deposition time.....36
Table 3. Variation of H_c , M_s , Sq and M_r with different annealing temperatures.....38.

ABSTRACT

In recent years, BaM ($\text{BaFe}_{12}\text{O}_{19}$) are the most interesting topic in the research because of its application in magnetic recording media, microwave devices and millimeter wave devices. It shows high resistivity, high chemical stability and good magnetic properties. Recently, the focus of the researcher has been laid to the development of thin and thick films, owing to its versatile above mentioned properties. In the present work, $\text{BaFe}_{12}\text{O}_{19}$ thin films are prepared by magnetron sputtering technique. The main focus was to understand the effect of deposition time and annealing temperature on the structural and magnetic properties of $\text{BaFe}_{12}\text{O}_{19}$ thin films.

1.1 Classification of hexaferrites:

Type	Chemical Formula	
M-	$RFe_{12}O_{19}$	R = Ba, Sr, Pb
W	$RMe_2Fe_{16}O_{27}$	Me = Fe ⁺² , Ni ⁺² , Mn ⁺² etc.
X-	$R_2Me_2Fe_{28}O_{46}$	
Y-	$R_2Me_2Fe_{12}O_{22}$	
Z-	$R_3Me_2Fe_{24}O_{41}$	
U-	$R_4Me_2Fe_{36}O_{60}$	

1.2 Introduction of M-type hexaferrite:

From last few decades, hexaferrite is massively important material technologically and commercially due to its tailorable properties. Among the vastly available ferrite families, this proposal mainly focused on commercially enriched, easily available M-type hexaferrite, which dominates in the family of hexaferrites due to its large uniaxial magnetocrystalline field ($H_A \sim 17\text{Koe}$), self-biasing nature, high permittivity, permeability and low microwave losses [1]. BaM has been widely used in permanent magnets, magnetic sensors and microwave device applications. This also plays a vital role in commercial and military applications like radar absorbing materials and signal transducer etc. Numerous proposals have been proposed to enhance its uniaxial magnetocrystalline anisotropy (H_a) for high frequency microwave device application.

1.3 Structure and properties:

M-type ferrite has gained large technical importance because its characteristic magnetic properties lie in its magnetoplumbite crystal structure in which trivalent Fe^{3+} ions occupy three different crystallographic sites; 3 octahedral, 2 tetrahedral and 1 triangular bipyramidal sites respectively. Each unit cell of M-type ferrite is made up of S and R blocks giving the unit cell formula SRS^*R^* , where * represents the mirror image of S and R blocks i.e. block rotates through 180° . Moreover, substitution of the magnetic ions with the non-magnetic ions remarkably changes the magnetic properties of the M-type hexaferrite. For example, substitution of indium reduces the H_a and shifts the FMR frequency. However, substitution of Al and Ga gives

rise the H_a value and also shift its operational frequency upto W band[2]. Hence, by suitable substitution M-type hexaferrites can be used in the wide frequency range (1-100GHz)[3].

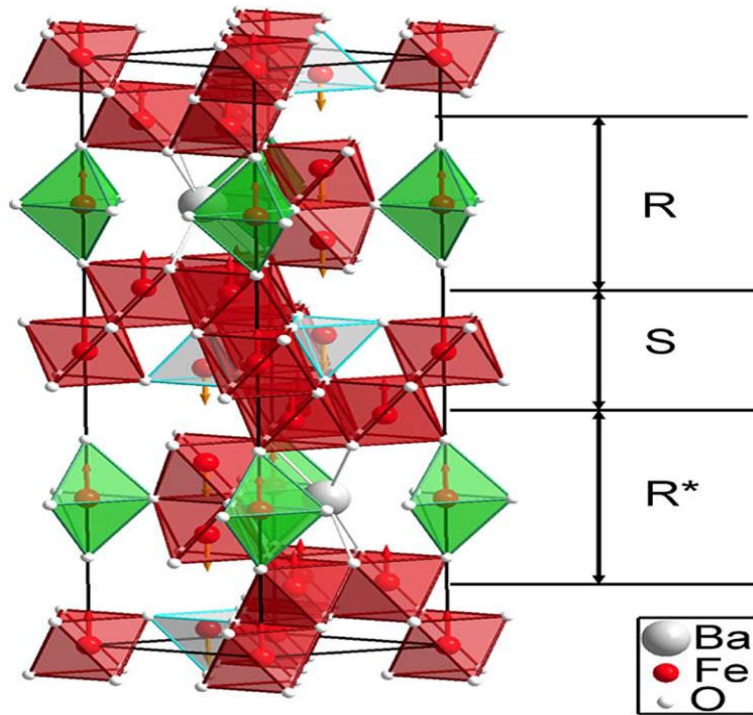


Figure 1.2 Magnetoplumbite structure

1.4 Synthesizing techniques for hexagonal ferrites:

There are various type of methods to process hard ferrites which can classify in major three types:

1. High Energy Ball Milling Method
2. Sol-Gel Method
3. Chemical Co-precipitation Methods

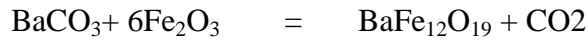
Among the various processing technique solid state is most widely used. The basic principle of the solid state method is diffusion process.

1.4.1 Solid State Synthesis Method: The basic steps for solid state synthesis are mentioned below:

1. Mixing: Precursors are mixed together in stoichiometric composition to get homogenous mixture that can be achieved either by using wet mixing or by dry mixing. Acetone, hexane or

water can be used as wet media. In wet mixing ball mill, zirconium jar and zirconium balls are used.

2. Calcination: As obtained homogeneous mixture are heated at high temperature called calcination process. Phase formation is done at the particular calcination temperature. At low calcination temperature pure BaM phases is not formed, even at high temperature excessive grain growth occurs and coarse grain BaM is formed.

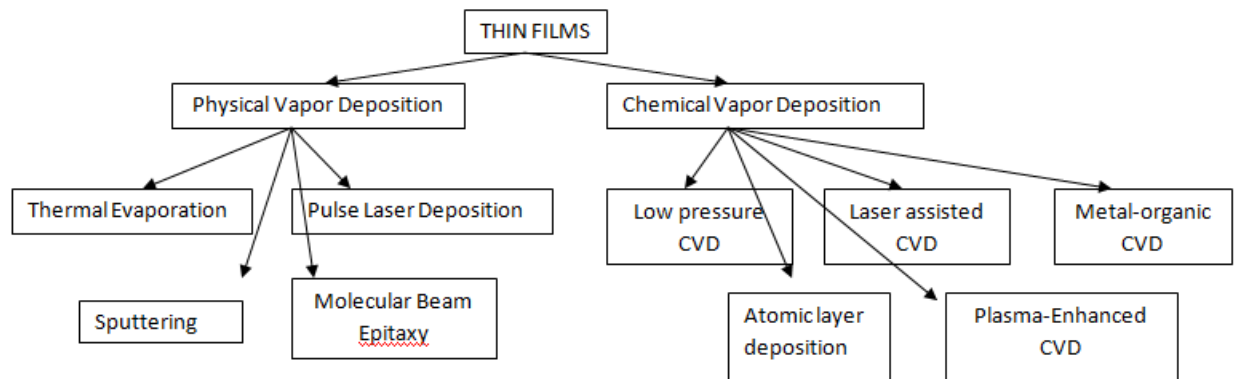


3. Wet grinding: In this process, the calcined powders/pellet are wet grounded using ball milling to get the uniform particle size. RPM and ball-to-charge ratio are generally kept fixed. Particle size from 0.7-0.9 μm shows good magnetic properties, whereas broad particle size distribution leads to abnormal grain growth which affects the magnetic properties of the materials.

4. Sintering: Sintering is carried out to obtain bonding between the particles and for effective densification. During the sintering process grain size increases but care is taken to avoid excessive grain coarsening.

1.5 Thin films deposition techniques

Thin films can be prepared by various techniques. The methods used for the deposition of thin films are given below in the form of flow chart.



Flowchart 1 Thin film deposition techniques

1.6 Physical vapour deposition:

Physical vapour deposition is a technique in which the source materials is converted from the condensed state to vapour state and then again convert in solid form when it comes in contact with the substrate[4]. In this way, a thin layer of source materials develops on the substrate surface. Processes based on this principle are:

- Pulse laser deposition
- Thermal evaporation

Sputtering1.6.1 Pulse laser deposition:

Lasers have been used because it is very good way to get high temperature and high density plasma[5]. This high temperature vaporizes the target materials. This may rise to three different processes such as

1. Laser interaction with the target material and evaporation occur
2. Laser interaction with the evaporated material and 3d expansion
3. deposition of the thin film[5].

This technique is widely used to fabricate high dense uniform thin film with the slow rate deposition.

Advantages:

1. High dense uniform film
2. Target size and shape never affect the film

Disadvantages:

1. Experimental set is costly.
2. Slow rate deposition makes thick film of micrometer order is experimentally impossible.

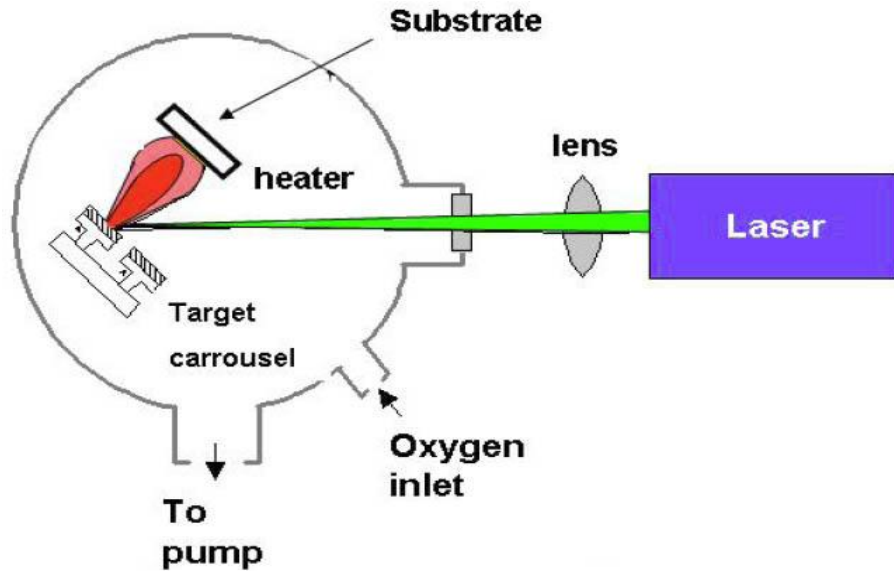


Figure 1.3 Pulse laser deposition

1.6.2 Thermal evaporation:

In this process, Vaporization of solid materials occurs when heated to sufficiently high temperature and condensation of the vapor onto cooler substrates yields thin solid films. The deposition usually carried in vacuum which helps the enhancement of the films. Few grams of material is required as a target. Due to its simple and efficient methodology this is used widely to fabricate solar cells, thin film transistors and UV protected glass etc.

Advantages:

1. Cost efficient
2. No need to go for sophisticated target preparation few grams of powder, foil and pellets required.

Disadvantage:

1. Less interaction between substrate and film
2. High chance of contamination and non-uniform films.

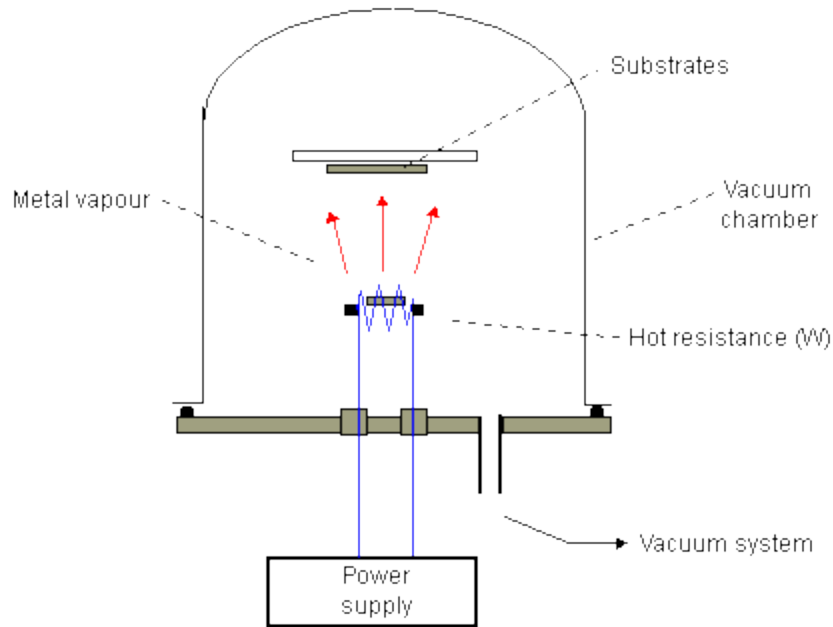


Figure 1.4 Thermal evaporation

1.6.3 Sputtering:

Sputtering is the widely used technique for thin film deposition. In this method particles are ejected from the target material due to the bombardment of high energy particles (plasma) and deposit on the substrate surface. It can be done by two processes:

- Radio frequency (RF) sputtering
- Direct current (DC) sputtering

RF sputtering: In the RF sputtering process, the target material, substrate, and RF electrodes begin in a vacuum chamber. Next, the inert gas, which is usually argon, neon, or krypton, depending on the size of the target material's molecules, is directed into the chamber. The RF power source is then turned on, sending radio waves through the plasma to ionize the gas atoms. Once the ions begin to contact the target material, it is broken into small pieces that travel to the substrate and begin to form a coating.

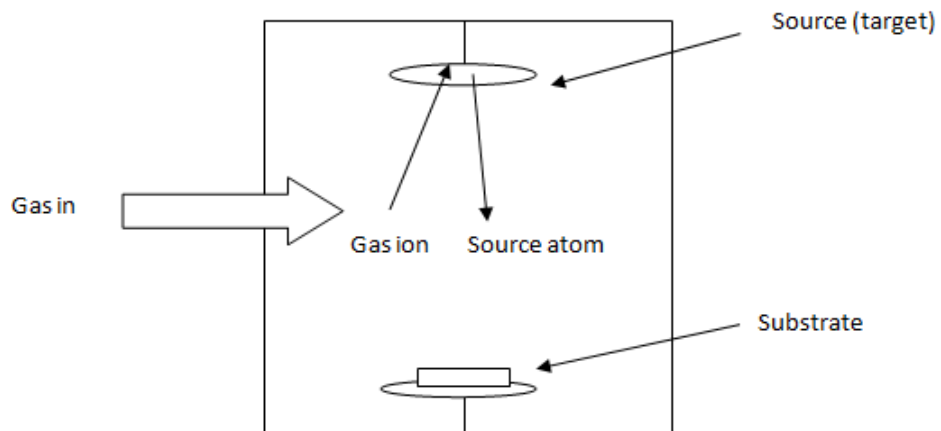


Figure 1.5Sputtering

Advantages:

1. No limitation on melting point.
2. Adhesion with the substrate in this process is more than thermal evaporation.
3. Uniformity of the film is better.

Disadvantage

1. High vacuum is required.
2. Required high maintenance due to chance of high contamination.

DC Sputtering:DC sputtering is done with conducting materials.Magnets are used to increase the percentage of electrons that take part in ionization and increase the probability of electrons striking the argon atoms.

Chapter 2

Literature review

A large amount of work has been carried out on BaM thin film deposited by different deposition technique. The section below summaries the important work carried out on pure and substituted BaM thin film deposited by adopting different methodology.

In 1990, P.Gerard observed the effect of heating on the properties of BaM thin films. He observed that the intermediate layers converted from magnetite to maghemite which are mainly responsible for c-axis orientation[6]. In 1990, the same year Dennis E. SPELIOTIS observed the peak shift in the BaM thin films. He observed that peak shift basically depends upon the thickness of the film. As the thickness increases, peak shift is decreases[7]. After that In 1994, Akimitsu Morisako deposit the hexaferrites films at low temperature and analyze the effect of the substitution of Pb on the properties of the hexaferrites films. He observed that Pb substitution facilitates the crystallization and increases the crystallinity. Also, Pb substituted films have more c-axis orientation. With the Pb substitution films H_c and saturation magnetization (M) were changes from 0.7 to 1.0 kOe and 250 to 300 emu/cm³ respectively[8]. In 1994 same year, N. Matsushita deposited the BaM thin film of thickness 500nm with ZnO underlayer at 600deg C by using Xe and Ar gaspressure of 0.10 Pa. In this paper he compared the magnetic properties of thin films prepared in different gas atmosphere. He did coating with mixture of Ar+O₂+Xe gas and another was mixture of Xe+O₂. He observed that coating in the atmosphere of Xe+O₂ is good. Coating by using Xe showed M_s , $H_c(\text{perp})$, $H_c(\text{paral})$ is 293 emu/cm³, 2.0 and 0.3 kOe respectively. On the other hand, for Ar atmosphere we get observed M_s and $H_c(\text{parall})$ were 196 emu/cm³ and 0.6kOe respectively. Xe atmosphere also give good crystallinity and magnetic characteristics for the coating on the ZnO underlayer[9]. In 1994, Jinshan Li explain the properties of the BaM thin films deposited on the carbon substrate which was pre-coated with silicon nitride. As obtained thin films were annealed at 640°C. SEM micrographs showed that we can control the grain size by changing the thickness of the film. As the thickness reach up to 10 nm, interdiffusion layer between BaM and silicon nitride under layer give initiate to randomly oriented BaM gains[10]. In 1995, Jinshan and Robert Sinclair analyze the texture of BaM thin films deposited on the ZnO underlayer. ZnO underlayer helps to get better c-axis orientation with because ZnO under layer

react with BaM and form intermediate layer of $ZnFe_2O_4$ which reduces the lattice mismatch between BaM and ZnO. XRD plots showed that film deposited with ZnO underlayer shows dispersion angle of 0.2° . [11]. In 1995, B. Ramamurthy studied the effect of the rate of annealing on the properties of the strontium hexaferrite thin films. In this paper they did thin films were deposited by rf-sputtering on fused quartz substrates with two different RF powers 60W and 330W. $M-H$ loop for thin film prepared by using RF power 60W was same for both fast annealing and slow annealing. But as we increase the power to 330W, c-axis which was perpendicular to the plane of the thin film shows random direction. And $M-H$ loop shows different behavior for both annealing rate. For slow annealing process M decreases because Fe_2O_3 phase formed and that phase shows non-magnetic character. However, fast annealing films shows 110 and 220 peaks with c axis in the plane of film [12]. In 1996, R. Chandrasekhar studied the properties of the sandwich type BaM thin films. In his paper they study the effect of BaM films were deposited on Pt underlayer silicon wafer coated with SiO_2 . These type of films shows good saturation value, H_c and squareness [13]. In 1996, Akimitsu Morisako studied the properties of the post annealed BaM thin films. Substrate temperature vary from room temperature to $500^\circ C$ and effect of the annealing temperature on the H_c of the thin film were reported. As the annealing temperature of the thin film increase from $650^\circ C$ to $900^\circ C$, the H_c increases from 1.0 to 3.8 kOe [14]. In 1997, Yingjian Chen studied the effect of the Ba content on the grain size and crystallization of the BaM thin films. Films with low Ba content show one dimensional and films with high Ba content show two dimensional growth. Also, Low Ba content film show more crystallinity than high Ba content films. It's because of high Ba content films has more nucleation sites than low Ba content films [15]. In 1998, B. X. GU studied the effect of the Co substitution in BaM thin films on the structure and magnetic properties. Co and Ti substituted BaM hexa-ferrite thin films shows large squareness and its value is 0.68 at room temperature [16]. In 1998, Chih-Ming Kuo studied the effect of Co and Sn doping on the thermal stability of the magnetic properties of BaM thin films. Co/Sn substitution in the BaM thin film cause a decreases in M_s , $H_c(\text{perp})$ and $H_c(\text{parall})$. Films in-plane and out of plane H_c remain constant between $20^\circ C$ to $100^\circ C$ [17]. 1998, A. Morisako study the effect of oxygen pressure on the properties of BaM thin films. Smoothness of the film and deviation from the perpendicular c-axis depends upon the oxygen pressure. Thin films were deposited at three different oxygen pressures; below 0.003mTorr, 0.003-0.2mTorr and 0.3-3.7mTorr. At low oxygen pressure rough

surface films with spinel like structure was obtained. But for the high oxygen pressure spinel + BaM phases and pure BaM phase were formed respectively. At large oxygen pressure, high perpendicular H_c and needle like structure were obtained. on the other hand, for 0.003-0.2mTorr pressure smooth surface and high perpendicular H_c of the films were observed[18]. In 1999, Xiaoxi Liu reported the properties of the BaM thin films prepared by alternate deposition by changing the Ba content in it. Films with high Ba content shows their easy axis of magnetization lies perpendicular to the plane and for those with low Ba content shows their easy axis of magnetization lies along the plane of the thin film. The change in H_c with changing temperature were observed. Effect of the temperature on H_c in high Ba content thin films, is more as compare to low Ba content thin films[19]. In 2000, Xiaoxi Liu studied the effect of the substitution of La and Zn on the properties of strontium hexaferrite thin films. Increase in M upon suitable amount of La-Zn substitution was reported. Substitution also effect the change in H_c by changing the temperature but by proper amount of substitution of La-Zn we can reduce the temperature effect on H_c [20]. In 2000, J. Feng studied the effect of Al substitution and addition of SiO_2 on the properties of the BaM thin films. By changing the amount and type of the substitution, the change in H_c and squareness of thin films has been observed. With the addition of small amount of SiO_2 ; perpendicular H_c and squareness increases but M decreases by 15%. Al substitution also follow the same trend but the H_c in the case of SiO_2 substitution is more as compare to Al substitution[21]. In 2000, M.E. Koleva studied the properties of the strontium hexaferrite thin films prepared by pulsed laser deposition technique. He observed that as the thickness of the thin film increases, it shows large c-axis orientation and decrease in the thickness give rise to the M . He showed that a film of thickness 750nm has good c-axis orientation, high M and high H_c [22]. In 2001, S. Nakagawa studied the effect of film thickness on magnetic properties of BaM thin films deposited with Pt underlayer. He observed that as the thickness decreases, film shows more and more c-axis orientation but as the thickness goes below 60nm, the perpendicular H_c decreases. Thickness of the films also affects the crystallite size and grain size. As the thickness decrease from 60nm to 8nm, it changes the crystallite size from 19nm to 7nm and grain size 80nm to 40nm[23]. In 2004, S. Capraro studied the properties of the BaM thin films deposited by sputtering. Films having thickness 1-10 micrometer deposited on the silicon substrate or glass substrate shows smooth surface and good uniformity in depth. Films annealed at low temperature shows amorphous characteristics and as the annealing temperature increases

crystalline character of the film increases[24]. In the same year he again analyzes the effect of annealing temperature, substrate temperature and RF power on the nature of BaM thin films. He observed that those films which deposited at low RF power shows good crystallization and preferential orientation among the planes (101),(200),(203),(102),(110) and (205) [25]. In 2005, Safia Anjum studied the effect of different kind of annealing. He explained the two types of annealing, one is called in-situ annealing and another one is called external annealing. In most of the cases to obtain the thick film by sputtering method is difficult because if we use the multilayer method to form a thick film it will take large time, on the other hand, in-situ annealing after every deposition film we heat the film at suitable annealing temperatures instantly and then do the next coating. In this paper they showed that both types of annealing have no effect on the H_c of the films as well as on squareness. M in the case of in-situ annealing is higher than in external annealing process. In-situ process has H_c 3.5kOe and M is 4.0 K gauss[26].In 2010, Huizhong Xu deposited M-type ferrite thin films on sapphire substrate by rf sputtering. 500nm thin films were deposited by changing the pressure from 0.2 to 1 Pa. With the pressure,atomic ratio of Fe to Ba increased from 9.3 to 15.0. XRD patterns confirmed that c-axis of all the films are perpendicular to the film plane. On the surface of the films, needle like grains are observed which corresponds to the high magnetocrystalline(H_a) of the films. At high pressure large number of needle like crystallites on the surface of the film observed which are parallel to the c-axis of the film and nucleation with the c axis normal to the film deteriorates [27]. In 2010, Wenxu Zhang deposited the BaM thin filmson sapphire substrate to study the effect on H_c . The experimental results showed that films which are deposited at room temperature have high H_c of the order of 11.5kOe. Grain size of 0.2 μ m was observed from the AFM micrographwhich is below the critical domain size of BaM. The MFM images showed that stray magnetic field in the remanent state is due to the isotropic assembly of domains[28]. In 2011, H. Hassane studied the magnetron effect on BaM thin films. He observed that all films deposited at different positions, under the same magnet, show different properties like thickness and roughness. Most of times, a single film shows different properties, even at different areas of the same film. So he mentioned three types of zones lies on the surface of the film called E-zone, M-zone and I-zone. Thickness of the film vary from highest to lowest ,as we go from M-zone to E-zone and I-zone has the lowest thickness. Roughness also follow the same trend[29]. In 2011, S.M. Masoudpanah studied the effect of oxygen pressure on the properties of strontium hexaferrite thin films deposited on

silicon wafer with Pt underlayer by pulse laser deposition. As the oxygen pressure increases, it gives rise to the perpendicular H_c and squareness. When the oxygen pressure was kept at 0.13mbar, the obtained M and anisotropic field values were equal to bulk[18]. In 2012, S.M. Masoudpanah reported the effect of thickness on the properties of strontium hexaferrite thin films deposited by pulse laser deposition. There was decrease in coercivity with increase in film thickness. This decrease in H_c is due to the increase in the grain size and relaxation in the lattice strain. If the thickness of the film is very low then it will disperse the c-axis. This dispersion of the c-axis is because of strain in film. As the thickness of the film increases, it reduces the strain that results in less dispersion in the c-axis[30]. In 2012, Safia Anjum studied the parallel H_a of BaM thin films. He also explained the effect of substrate temperature on the properties of the film. If the temperature of the substrate is low then it restricts the formation of the larger grains and it does not show H_a . As the temperature of the substrate increases, easy axis changes from perpendicular direction to the in plane direction. However, hard axis always remains in the perpendicular direction. Higher substrate temperature showed uniaxial H_a which is necessary for magnetic recording media[26]. In 2013, S.M. Masoudpanah reported the effect of different metal precursors on the magnetic properties of $\text{SrFe}_{12}\text{O}_{19}$. Different metal precursor has different effect on the magnetic properties of the thin film like M and H_c . Films which were synthesized from metal nitrates obtained magnetization and H_c were 267 emu/cm^3 and 4790 Oe respectively. On the other hand, film synthesized from metal hydroxide and metal chloride precursor have H_c 6063 and 55047 Oe respectively, however, M was low i.e. 215 and 171 emu/cm^3 respectively[31]. In 2013, M. Khaleeq-Ur-Rahman reported the effect of external magnetic field on the properties of strontium hexaferrite thin films deposited by pulse laser deposition. He observed that magneto-optical properties of the film improve at higher temperature in the presence of external magnetic field. The external applied magnetic field also increases the saturation magnetic field, retentivity and refractive index of the films but decreases the absorption power of the material[32]. In 2013, S.M. Masoudpana reported the effect of SrFeO underlayer and deposition temperature on the properties of strontium hexaferrite thin films deposited by pulse laser deposition. The results showed that SrFeO underlayer always helps to get the easy axis of magnetization perpendicular to the plane which is responsible for large perpendicular H_a and high H_c . As the coating temperature of the SrFeO underlayer increases, M and H_c of the thin film increases. Upto a certain limit of temperature it starts decreases[33]. In 2015, T. Garcia studied

the effect of annealing temperature on magnetic properties of strontium hexaferrite thin films deposited by pulse laser deposition. He observed that if the annealing temperature is 600°C or below, then film showed very weak magnetic behavior. If the annealing temperature is more than 700°C then it become nanocrystalline particle system and behaves as one domain system and show excellent magnetic property. He got 5750-6850 Oe H_c which is the highest in the thin films[34]. In 2015, Ke Sun studied the properties of thin films having different structures. He took three different combination, first was d_{s100} (single layer 100nm thick), second was d_{s200} (single layer 200nm thick) and third was d_{b200} was (bilayer of 200nm thick). All the films were deposited on the sapphire. He observed that d_{s100} films have platelet like grains with good magnetocrystalline(H_a) and squareness(0.62). While in d_{s200} acicular grains were formed which changes the c-axis from perpendicular to in- plane. Now best properties were obtained in d_{b200} . It has platelet like grains showing highest H_c and squareness of 0.67 and 98.6 kA/m respectively[35].

Table 2 Literature review summary

Year	Author	Study	Results
1995	Jinshan Li[11]	Effect of the ZnO under layer Gas=Ar+O2 Total pressure=3mtorr Substrate temperature=640°C	ZnO give better out of plane c axis orientation.
1995	Yoichi Hoshi [36]	Effect of ZnO under layer For ZnO Layer Substrate temperature 200-350°C Thickness=100-300nm Pressure= $5 \cdot 10^{-3}$ Pa Input voltage=450-530V Current=50mA Gas=80% O2+20% Ar For BaM film substrate temperature=560-640°C thickness=100-300nm pressure= $3 \cdot 10^{-3}$ Pa input voltage=560-640°C GAS=5% O2-95% Ar	Crystallite size increases up to 2000°C with ZnO underlayer; it also increases H_c and gives good c-axis orientation.

1997	Y.Hoshi[37]	1.Effect of the ZnO under layer 2. thickness effect on crystallite size Substrate=silicon Gas=2%O ₂ +98%Ar Substrate temperature=580°C Voltage=680V Thickness=10-200nm	1. ZnO increases the c-axis orientation, decreases in the H _c and M. 2. As the thickness decreases the crystallite size also decreases and it decreases the coercive force and magnetization of the film.
1988	A.Morisako[18]	Effect of the oxygen pressure Range: 0.003mtorr 0.003-0.2mtorr 0.3-3.7 mtorr	Only 0.003-0.2 mtorr shows good magnetism and smooth surface
1988	E.Lacroix[38]	Effect of the annealing temperature Total pressure=8mtorr Background pressure=10 ⁻⁶ Pa Substrate temperature=400°C	At low annealing temperature films shows amorphous characteristics. Annealing temperature about 800°C shows good properties.
1999	A.Morisako[39]	Effect on film composition by using Different targets having different ratio(N) of Fe/Sr Gas= Ar+O ₂ Total pressure= 2mtorr Oxygen pressure= 0.2mtorr Substrate temperature=600°C Thickness= 150nm	1. For N=8 shows rice like grains on the other hand for N=10 it is of chunk like shape. 2. for N=8 shows maximum M _s and H _c if we increases N both M _s and M _r first decreases and then remain constant. 3. for N=10 we get highest f _c (orientation factor).
1999	T.S.Cho[40]	Effect of the thickness on the properties BaM Substrate=sapphire Gas=Ar+10%O ₂ Annealing temperature=750°C Time=5 hour RF power= 1W/cm ²	As the thickness decreases the H _c (in-plane) decreases but (out-plane) H _c shows little change. On the other hand, M for (out plane) increases but in-plane shows little decrease.
2000	Akimitsu Morisako[41]	Effect of the Cr addition on the properties of the BaM thin films Substrate= silicon Pressure=2mtorr Gas=Ar+O ₂ Oxygen pressure= 0.2 mtorr Substrate temperature=550°C Power=40W Thickness=150nm	1.M and H _c is decreases as Cr content increases. 2. orientation factor increases with increases in the Cr content.

2000	Xiaoxi Liu[20]	Effect of the La-Zn Substitution on properties of SrM films. (La-Zn) _x Sr _{1-x} Fe _{12-x} O ₁₉ Thickness=150nm Annealing temperature=750°C Time=1 hour	1. H _c and M both are increases with increases in the La-Zn content. 2. Curie temperature decreases as substitution increases. 3. parameters a and c both are decreases with increases in the content.
2001	Shigeki Nakagawa[23]	Effect of Pt underlayer Substrate=silicon Substrate temperature For Pt layer=300°C For BaM layer= 500°C Pt thickness=15nm Ar pressure=1.99mtorr O ₂ pressure= 0.01 mtorr	1. Pt under layer shows good c-axis orientation. 2. Perpendicular H _c decreases below 60nm thickness OF BaM thin film but multilayer of (BaM/Pt) _n shows high H _c at low thickness also
2002	P.HING[42]	1. effect of the annealing temperature (700-1000°C) 2. effect of sputtering pressure 3. effect of oxygen flow rate	1. H _c increases 2. up to 15mtorr M _s and H _c both increases 3. M _s decrease as oxygen flow increases but first H _c increases after certain point it starts decreases.
2002	B.Bayard[43]	Effect of different type of annealing Gas= Ar Pressure=0.1-1.2Pa Background pressure=10 ⁻⁴ Pa Annealing=600-800°C RF power=0-200W	Films depositing at room temperature shows amorphous characteristic. Rapid thermal annealing and classical thermal annealing shows same properties.
2003	S.Capraro[44]	Effect of the different rate of annealing Fast annealing(RTA) =100°C/min Slow annealing(CTA) =7°C/min Gas=Ar Base pressure=8*10 ⁻⁵ Pa RF power= 50 & 100 W	Coercive force is higher for CTA. M and M _r is higher for RTA. Films show good magnetic properties for 800°C and for low RF power 50W.
2004	S.Capraro[24]	Effect of the different substrates and different annealing temperatures Pressure=5*10 ⁻⁵ Pa RF power=50-100W Distance between target and substrate=4.6cm Annealing temperature=800°C	At low annealing temperature films shows amorphous characteristics. Annealing temperature about 800°C shows good properties. 2. Residual stress for alumina substrate is less

			than silicon substrate.
2005	A.R.Abuzir[45]	Effect of the two different type of annealing(in-situ and external) Substrate=silicon Pressure= 3×10^{-6} torr Gas= Ar+O ₂ Substrate temperature=500-600°C D _{t-s} =6.3cm RF power=50W Pressure= 8×10^{-3} torr Annealing=950°C for 10 min	Out-plane H_c and squareness both are same for in-situ annealing and external annealing. Better c-axis orientation observed in external annealing.
2014	Akimitsu Morisako[8]	Effect of the Pb substitution Total Pressure=2.0mtorr Thickness=120nm Substrate temperature=400-600°C Oxygen pressure= 0.03mtorr	Pb substitution facilitates the crystallization. for substrate temperature above 460°C shows good c-axis orientation
2015	Xiaozhi zhang[46]	Effect of the oxygen content Ar+O ₂ (5-20%)	As the oxygen content increases it give rise the in-plane c-axis oriented films.
2016	Ke Sun[35]	Effect of different structure of BaM D _{s100} = single layer thickness 100nm D _{s200} =single layer thickness 200nm D _{b200} =bilayer thickness 200nm Pressure= 3×10^{-4} Pa Gas=1% O ₂ +99% Ar RF power= 140 W Film thickness=20nm Substrate temp=400°C	D _{s100} ,D _{s200} both shows platelet type grains which increases c-axis orientation and magneto anisotropy. D _{s200} shows less stress as compare to other BaM structural type.

CHAPTER 3

EXPERIMENTAL DETAILS

This chapter mainly describes the preparation of BaM powder, BaM target for sputtering and thin film preparation techniques. Further, different characterization techniques used are mentioned.

3.1 Preparation of BaM powder:

BaM powder was prepared by solid state synthesis method. To prepare BaM, analytical grade barium carbonate (BaCO_3) and iron oxide (Fe_2O_3) were used. Wet mixing of BaCO_3 and Fe_2O_3 in acetone media has been carried out using planetary ball milling for three hours. The ball to charge ratio and milling time was fixed to 2:1 and 3 hours respectively. The as-mixed powder was subsequently calcined at 1150°C for 6 hours in resistance furnace.



Figure 3.1 Ball mill



Figure 3.2 Vibratory mill



Figure 3.3 Furnace

3.2 Target preparation:

BaM target of 2 inch diameter was prepared from as synthesized powder. To get the good green compaction strength, the as-synthesized powder were thoroughly mixed with PVA (Polyvinyl alcohol) binder and dried overnight. The dried powder was grounded to free flowing powder using vibration mill and sieved from 45 mesh sieves. To pelletize the powder in the shape of circular target, powder was pressed using hydraulic press with the pressure of 600 kN at the rate

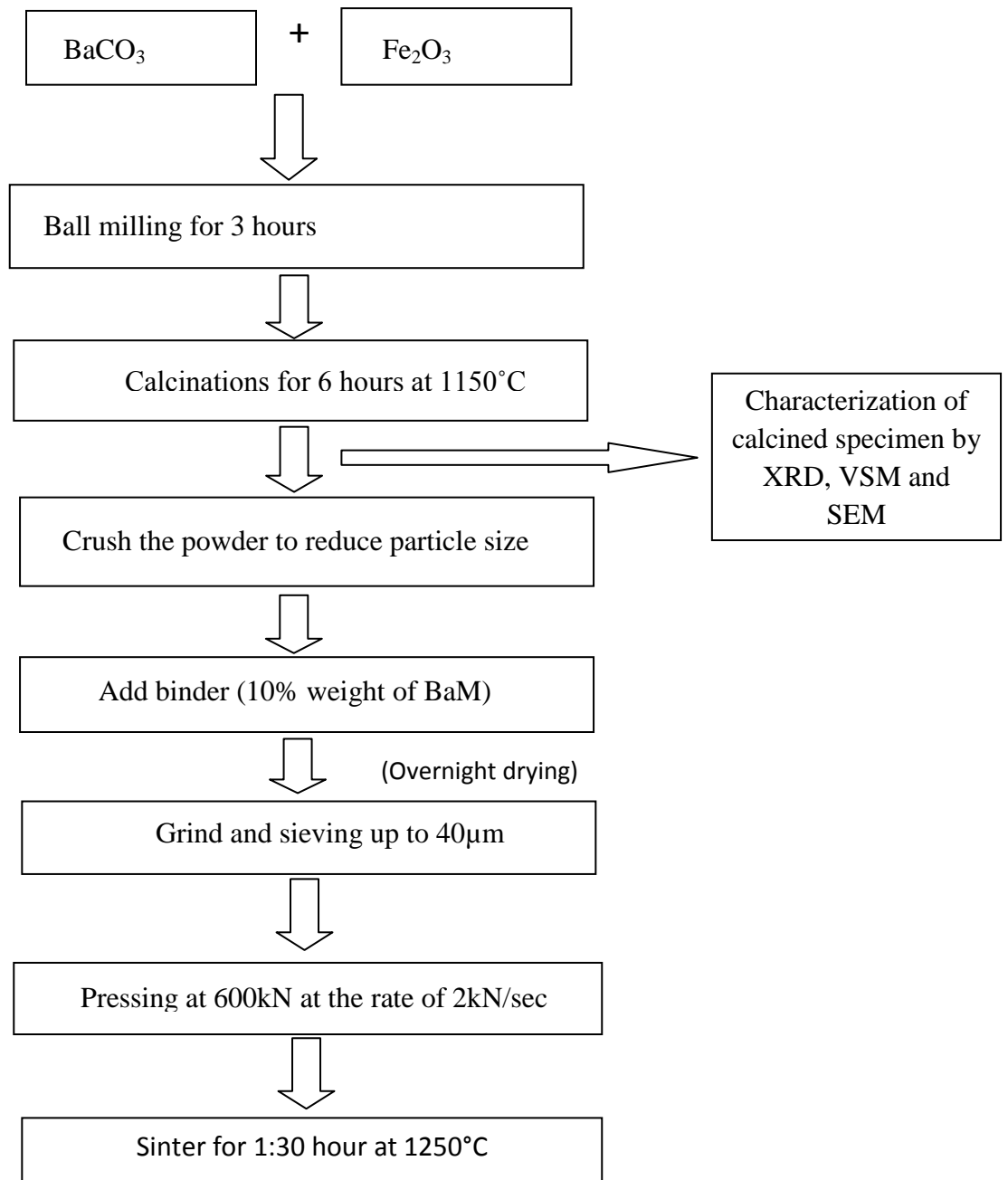
of 2kN/sec. To increase the density of the pellet, sintering was done for 1:30 hour at 1250°C in ambient atmosphere.



Figure 3.4 Pressing of BaM powder



Figure 3.5 BaM Target



Flowchart 2: Preparation of BaM Target

3.3 Thin film preparation:

As prepared BaM target was used for deposition of thin films. Thin films were deposited on Al_2O_3 substrate using rf-sputtering unit in the argon atmosphere. Target and substrate distance was kept constant to 5cm. The base pressure before introducing the argon gas was 5×10^{-5} mbar. Film has been deposited at the sputter pressure of 5×10^{-2} mbar for 15, 30, 45 and 60 min. respectively. As deposited films showed deep brown color. All the deposited films were annealed between the temperature range of 500°C to 1000°C .



Figure 3.6 Magnetron Sputtering unit

3.4 Characterization techniques:

Structural and magnetic measurements of BaM thinfilms were analyzed by X-ray diffractometer, scanning electron microscopy, vibration sample magnetometer.

X-ray diffraction (X'PERT Pro-Panalytical using $\text{Cu-K}\alpha$ radiation wavelength(1.5405 \AA) has been used to analyze phase formation. 2θ values vary from 30 to 35° .

Scanning electron microscope(SEM) is used to study the surface morphology at 2500x and 10000x. The model of the SEM used is JEOL (JSM-IT100).

Vibrating sample magnetometer (VSM) was used to study the magnetic properties of the BaM thin films. Model of the VSM used is Lake Shore 7404. Magnetization field for both powder and thin film was applied from -10000 to 10000 Oe. From the hysteresis loop we measure the M_s , M_r and H_c of the powder and as deposited thin films.

CHAPTER 4

Results and Discussion

4.1 Characterization of BaM powder

Fig. 4.1 shows the X-ray diffraction pattern of pure BaM powder prepared by solid-state synthesis route. All the diffraction peaks depicts the formation of single phase BaM without any secondary phase in the angle range 20° - 80° . It shows good agreement with JCPDS data (card no. 07-0276).

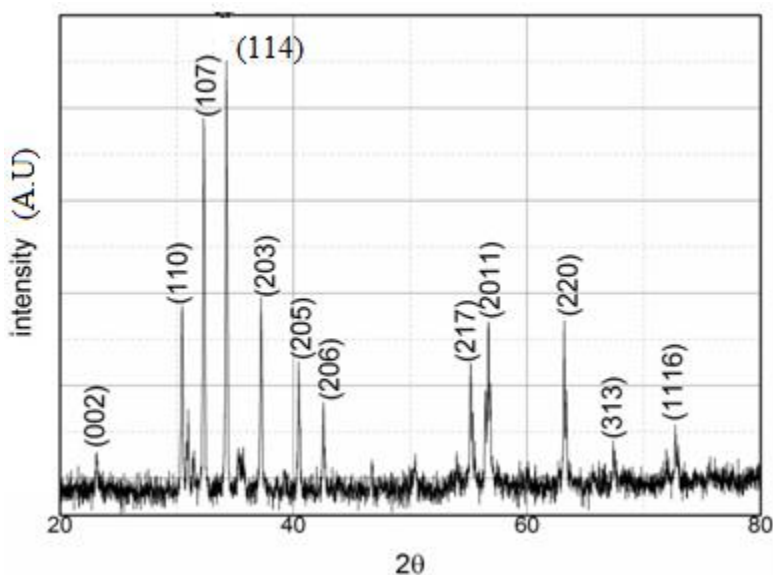


Figure 4.1 XRD pattern of pure BaM powder

Powder calcined at 1150°C . The micrograph shows multiple morphology with nearly uniform particle size. The Average particle size comes out to be $\approx 1.3\mu\text{m}$. fig. 4.2 (b) shows the corresponding EDS spectrum of the powder. The peak in EDS at different energy level represents the existence of Ba, O and Fe elements.

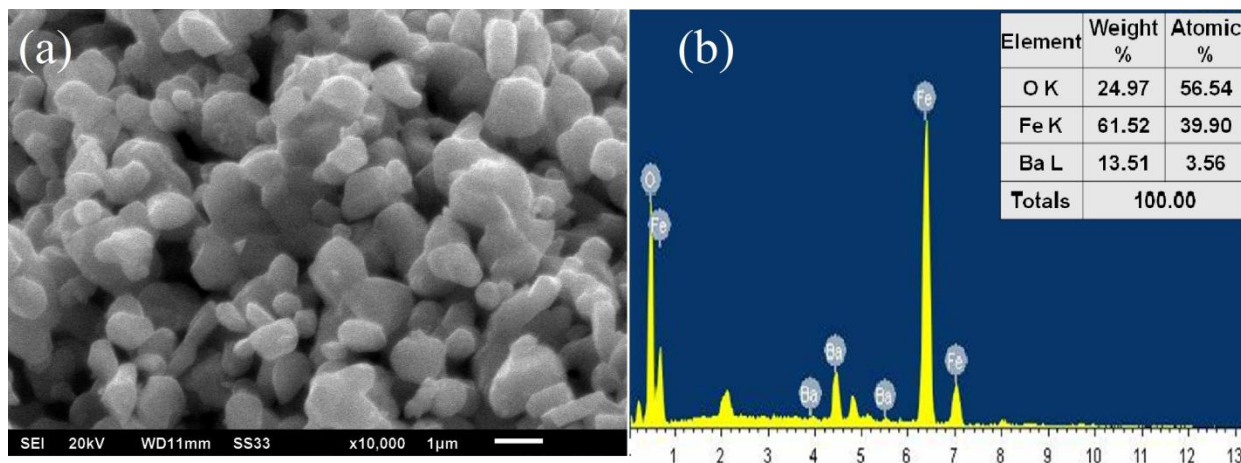


Figure 4.2(a-b) SEM micrograph and EDS analysis image of pure BaM powder

Magnetization curve (MH plot) of pure BaM powder is shown in fig.4.3. MH plot shows that BaM powder has high magnetization (~ 51.91 emu/g) at the applied field of 1T with moderate remanent magnetization of 32.83 emu/g and coercivity of 3445.97 Oe. Calculated squareness ratio comes to be 0.63 which shows good agreement with published results [47].

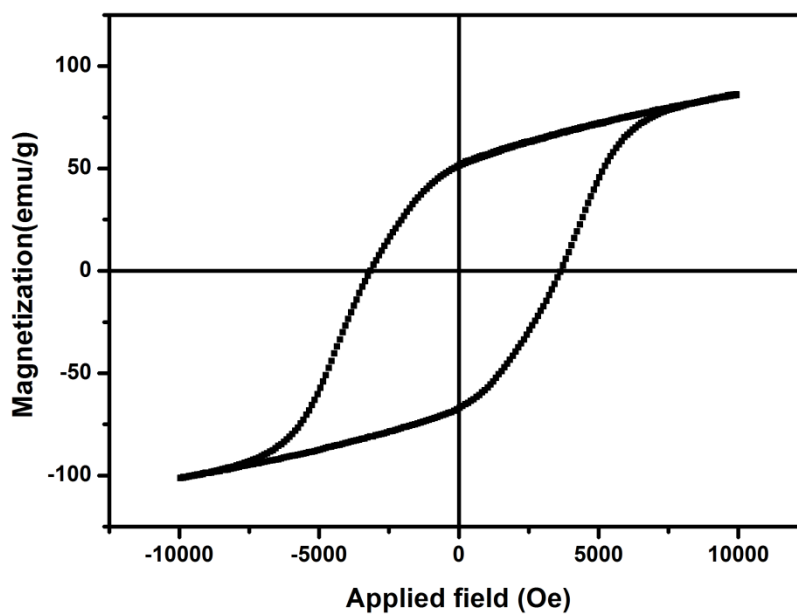


Figure 4.3 $M-H$ loop of pure BaM powder

4.2 Characterization of BaM thin films

The effect of deposition time and annealing temperature on the structural and magnetic properties of BaM thin films, X-ray diffraction (XRD) and vibrating sample magnetometer were employed.

4.2.1 Effect of deposition time:

Fig.4.4 represent the X-ray diffraction patterns of BaM thin films annealed at 1000 °C deposited for 15,30,45 and 60 min. respectively. Films deposited for 15 and 30 min shows a single peak (107) at 33.7°. However, for 45 and 60 min deposited films, along with (107) peak, (110), (112) and (114) peaks are obtained which corresponds to BaM peaks. The plot shows that crystallization improves with the rise in the deposition time.

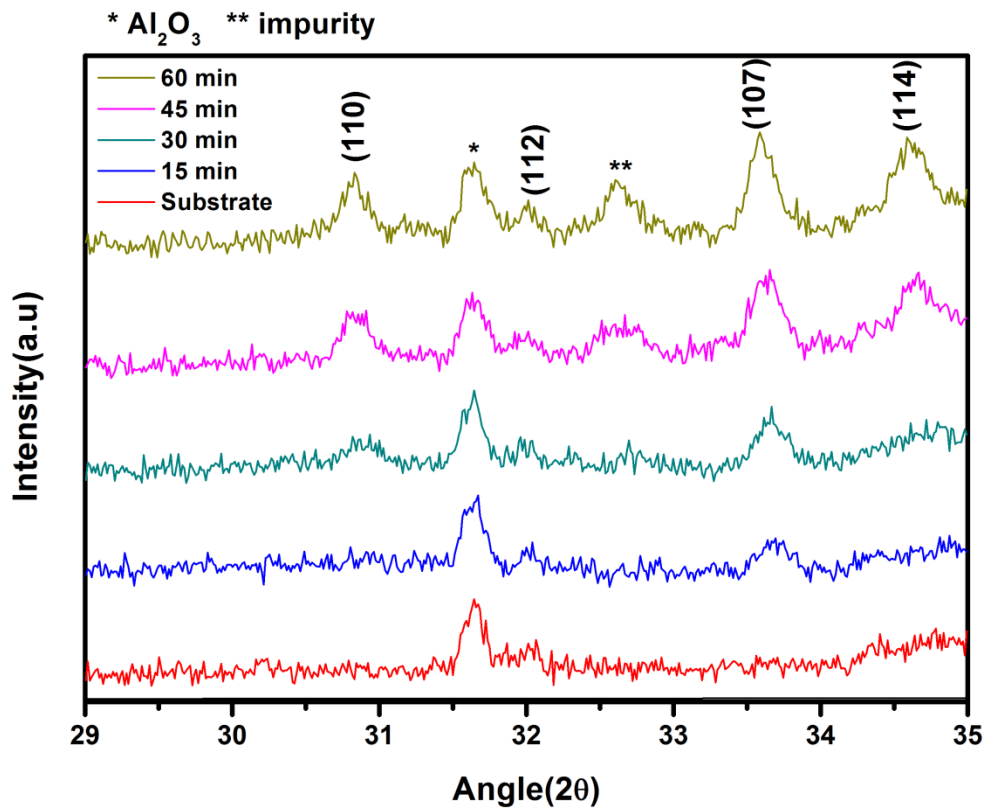


Figure 4.4 XRD patterns of BaM thin films for different deposition time

The in-plane (0°) and out of plane (90°) $M-H$ plots of sputtered films at different deposition time are shown in Fig. 4.5. With increasing the deposition time, a good $M-H$ loop with higher coercivity was observed which is similar to hard magnetic behavior. The thickness of the films increases with the deposition time which results the change in magnetic parameters. Change in magnetic properties coercivity H_c , magnetic moment (M_r , M_s) and squareness with the deposition time are tabulated in table 2. It explains the change in magnetic properties by changing deposition time.

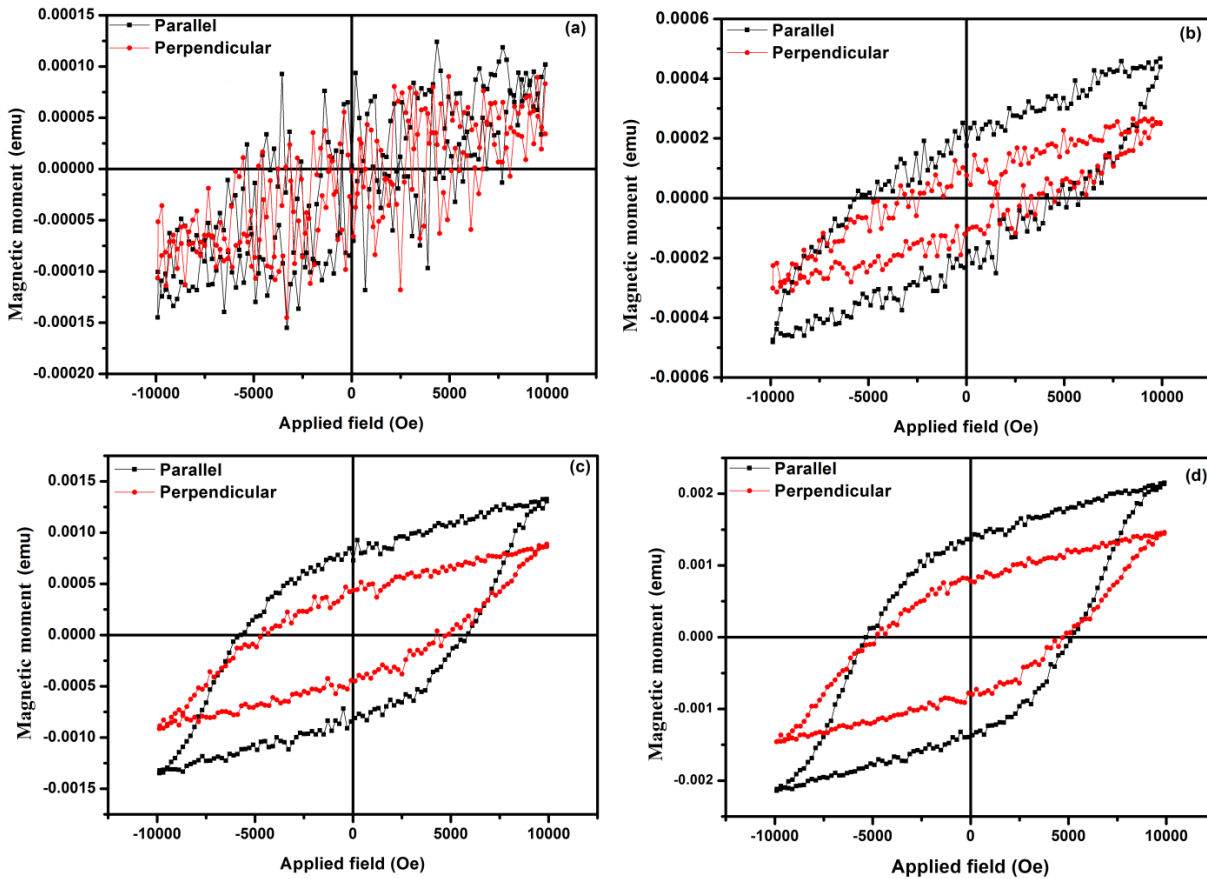


Figure 4.5 $M-H$ loops of (parallel and perpendicular) BaM thin films deposited for (a) 15 min (b) 30 min (c) 45 min (d) 60 min annealed at 1000°C

Table 2 Variation in H_c , M_r , M_s and Sq of BaM thin films for different deposition time

Deposition time(min)	Orientation	$H_c \cdot 10^2$ (Oe)	$M_r \cdot 10^{-4}$ (emu)	$M_s \cdot 10^{-4}$ (emu)	Squareness(sq)
30	0°	56.93	1.84	4.66	0.39
	90°	24.03	0.78	2.53	0.03
45	0°	57.06	7.50	13.21	0.56
	90°	46.62	7.50	8.87	0.84
60	0°	53.37	13.60	21.56	0.63
	90°	48.00	7.85	14.52	0.54

4.2.2 Effect of annealing temperature:

Fig.4.6 represents the X-ray diffraction patterns of 1 hour deposited BaM thin films annealed at 800,900 and 1000°C respectively. Phase analysis has been done with the help of Xpert's high score. As deposited films shows amorphous behavior and the film annealed at 800 °C showed the characteristic peak of substrate i.e. no characteristic peak of BaM has been observed. However, films annealed at 900 °C and 1000°C, all characteristic peaks correspond to BaM and the major peaks co-existing with JCPDS card 01-072-0738. A minor peak shift was observed for the films annealed at 900 and 1000 °C because of lattice mismatch between Al_2O_3 and BaM thin film.

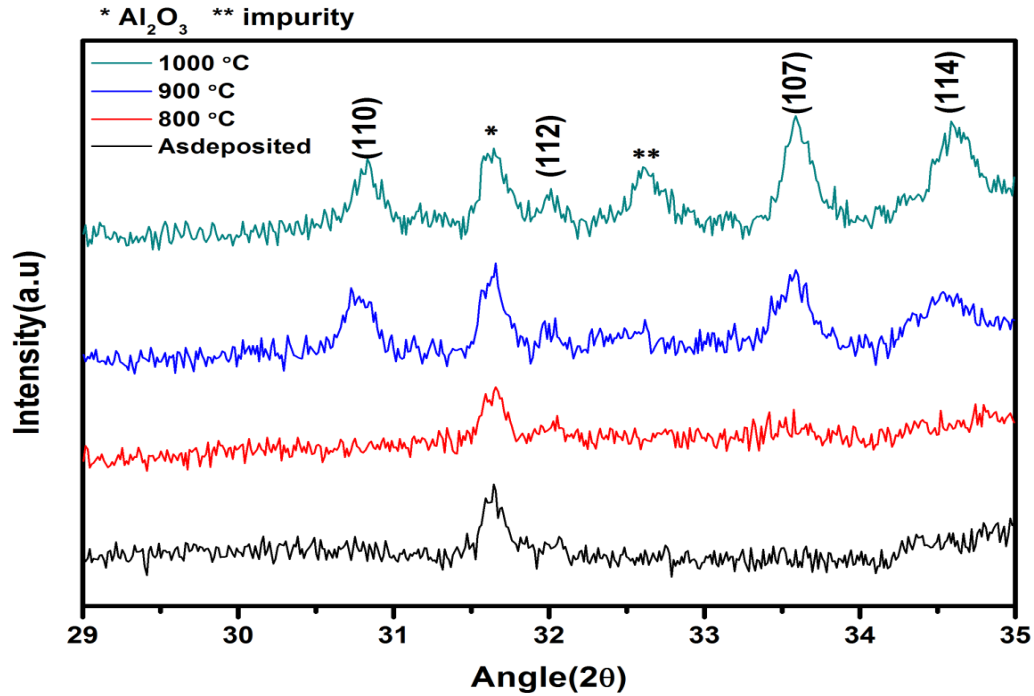


Figure 4.6 XRD patterns of BaM thin films for different annealing temperatures

The in-plane (0°) and out of plane (90°) $M-H$ plots of sputtered films annealed at different temperature are shown in fig. 4.7. The magnetization curve ensures that magnetic behavior improved with the annealing temperature. The paramagnetic behavior of the film at the lower temperature confirms the amorphous phase of the film as discussed in section 4.2.1.1 XRD. The drastic change in magnetic parameters is observed with annealing temperature. The good magnetic moment (M_r and M_s) and H_c were observed for the film annealed at 1000°C for one hour. The magnetic properties and squareness ratio are tabulated in table 3.

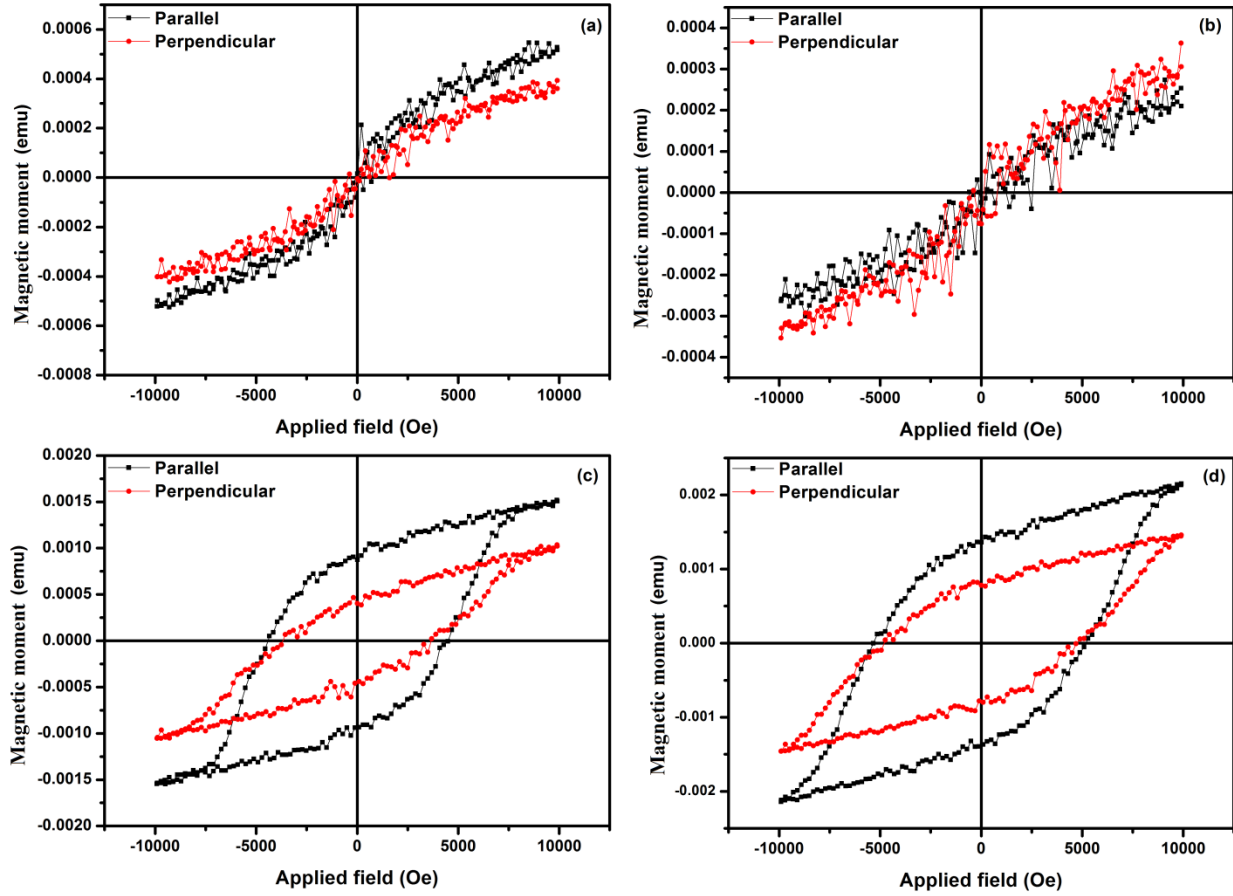


Figure 4.7 Hysteresis loopsof (in-plane and out-plane) 1 hour sputtered BaMthin films annealedat(a) 700°C (b) 800°C (c) 900°C (d) 1000°C

Table 3. Variation of H_c , M_s , Sq and M_r with different annealing temperatures

Annealing Temp.(°C)	Orientation	$H_c \cdot 10^2$ (Oe)	$M_r \cdot 10^{-4}$ (emu)	$M_s \cdot 10^{-4}$ (emu)	Squariness(sq)
500	0°	0.37	0.10	0.34	0.01
	90°	1.15	0.15	2.6	0.05
700	0°	0.68	0.13	5.27	0.02
	90°	0.37	0.07	3.93	0.01
800	0°	3.68	0.76	3.63	0.20
	90°	0.69	0.22	2.52	0.08
900	0°	44.14	8.79	15.13	0.58

	90°	36.66	4.08	10.32	0.39
1000	0°	53.37	13.60	21.56	0.63
	90°	48.00	7.85	14.52	0.54

Fig. 4.8(a-b) shows the SEM micrographs of BaM films deposited for 45 and 60 min and annealed at 1000 °C. The image ensures that the morphology of the film is affected by deposition time. The small amount of porosity has been observed in the film deposited for 45 min but not for the film deposited for 60 min. Hence film deposited at 60 min shows dense thin film and favorable for microwave application.

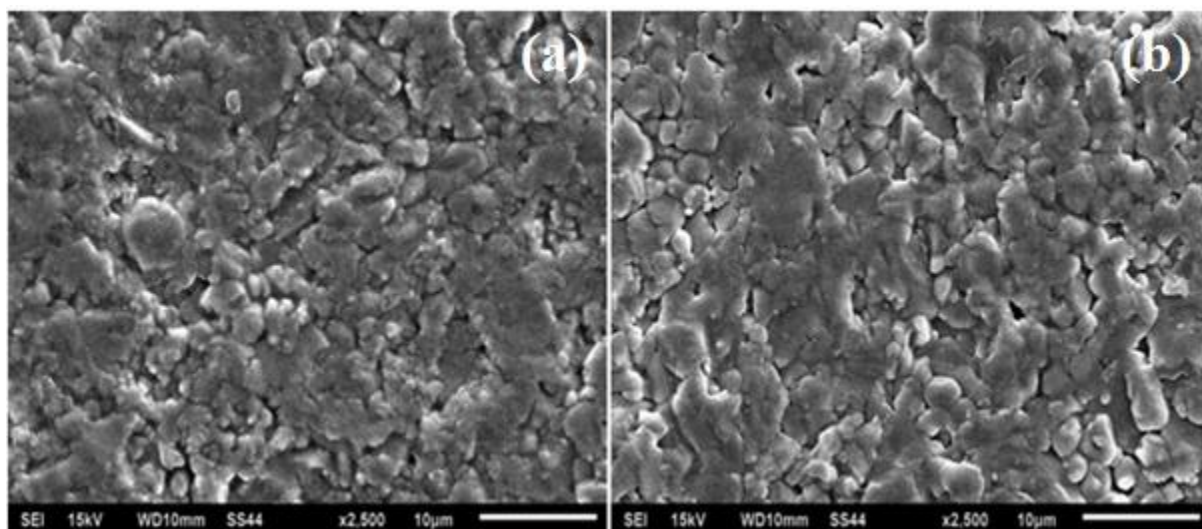


Figure 4.8 Surface morphology of BaM thin films deposited for (a) 45 min (b) 60 min annealed at 1000°C

Conclusion

We successfully deposited the thin films of BaM on the Al₂O₃ substrate by magnetron sputtering. The effect of the deposition time and annealing temperature on the crystallinity, microstructure and magnetic properties of the BaM thin films has been investigated. XRD patterns confirm that the crystallinity of the films has been improved with the deposition time as the most characteristic peaks of BaM was obtained for 60 min deposited film. Also the magnetic measurements (*MH* loop) for 60 min deposited film shows hard magnetic behavior with high coercivity as compared to 15, 30 and 45 min deposited thin films.

To study the effect of annealing temperature, all films deposited for 1 hour and annealed at 700, 800, 900 and 1000 °C respectively. For the films annealed at 700, 800 and 900 °C, poor crystallinity was observed along with poor magnetization behavior. However, the film annealed at 1000 °C shows good magnetization behavior along with high crystallinity and less porous microstructure.

Hence, we conclude that the deposition time as well as annealing temperature significantly affect the crystallinity, microstructure and enhance the magnetic parameters of the thin films.

References:

- [1] C. N. Chinnasamy, T. Sakai, S. Sivasubramanian, A. F. Yang, C. Vittoria, and V. G. Harris, "Magnetic and microwave properties of basal-plane oriented BaFe₁₁In₁₀O₁₉ ferrite thick films processed by screen printing," *J. Appl. Phys.*, vol. 103, no. 7, pp. 10–12, 2008.
- [2] S. Mahadevan, C. Pahwa, S. B. Narang, C. Pahwa, S. B. Narang, and P. Sharma, "Structural, dielectric and magnetic properties of BaFe_{12-x}Al_xO₁₉ hexaferrite thick films," *J. Magn. Magn. Mater.*, vol. 441 C, pp. 465–474, 2017.
- [3] L. G. Van Uitert and F. W. Swanekamp, "Permanent magnet oxides containing divalent metal ions. II," *J. Appl. Phys.*, vol. 28, no. 4, pp. 482–485, 1957.
- [4] N. Selvakumar and H. C. Barshilia, "Review of physical vapor deposited (PVD) spectrally selective coatings for mid-and high-temperature solar thermal applications," *Sol. Energy Mater. Sol. Cells*, vol. 98, pp. 1–23, 2012.
- [5] R. K. Singh and J. Narayan, "Pulsed-laser evaporation technique for deposition of thin films: Physics and theoretical model," *Phys. Rev. B*, vol. 41, no. 13, pp. 8843–8859, 1990.
- [6] P. Gerard, E. Lacroix, and M. Dupuy, "ANNEALING EFFECT ON THE PROPERTIES OF HEXAFERRITE FILMS OF CRYSTALLINE BARIUM AND B. BLANCHARD b, G. MAREST d, G. ROLLAND," vol. 83, pp. 13–14, 1990.
- [7] D. E. Speliotis, "Peak shift in particulate and thin film media," *J. Magn. Magn. Mater.*, vol. 83, no. 1–3, pp. 455–456, 1990.
- [8] A. Morisako, H. Nakanishi, M. Matsumoto, and M. Naoe, "Low-temperature deposition of hexagonal ferrite films by sputtering," *J. Appl. Phys.*, vol. 75, no. 10, pp. 5969–5971, 1994.
- [9] Y. Liu, M. G. B. Drew, Y. Liu, J. Wang, and M. Zhang, "Preparation and magnetic properties of La-Mn and La-Co doped barium hexaferrites prepared via an improved co-precipitation/molten salt method," *J. Magn. Magn. Mater.*, vol. 322, no. 21, pp. 3342–3345, 2010.
- [10] J. Li, R. Sinclair, S. S. Rosenblum, and H. Hayashi, "Characterization of Sputtered Barium Ferrite Thin Films on Silicon Nitride Coated Carbon Substrates," *MRS Proc.*, vol. 341, pp. 59–64, 1994.
- [11] J. Li, R. Sinclair, S. S. Rosenblum, and H. Hayashi, "Reaction-mediated texturing of barium ferrite magnetic thin films on ZnO underlayer," *J. Mater. Res.*, vol. 10, pp. 2343–2349, 1995.
- [12] B. R. Acharya, S. Prasad, N. Venkataramani, S. N. Shringi, and R. Krishnan, "The effect of deposition and annealing conditions on textured growth of sputter-deposited strontium ferrite films on different substrates," *J. Appl. Phys.*, vol. 79, no. 1, p. 478, 1996.
- [13] R. Chandrasekhar and D. J. Mapps, "Preparation and characterisation of sandwich type barium hexa-ferrite thin films," *J. Magn. Magn. Mater.*, vol. 157–158, pp. 326–328, 1996.

- [14] A. Morisako, M. Matsumoto, M. Naoe, and P. Electronics, "Crystallographic and Recording Characteristics of Post-Annealed Ba-Ferrite Sputtered Films," vol. 32, no. 5, pp. 3819–3821, 1996.
- [15] Y. Chen and D. Laughlin, "Influence of Ba content on grain size and dynamics of crystallization in barium ferrite thin films," *J. Appl. Phys.*, vol. 81, no. 8, pp. 4380–4382, 1997.
- [16] B. X. Gu, "Structure and Magnetic Properties of BaCoTiFe₁₀O₁₉ Thin Films with an Easy-Axis In-Plane Orientation," *J. Mater. Sci.*, vol. 33, no. 20, pp. 4987–4990, 1998.
- [17] P. C. Kuo and J. W. Chen, "Effect of Co/Sn doping on the thermal stability of magnetic properties of Ba-ferrite thin films," *IEEE Trans. Magn.*, vol. 34, no. 2, pp. 381–383, 1998.
- [18] A. Morisako, M. Matsumoto, and M. Naoe, "The effect of oxygen gas pressure on Ba-ferrite sputtered films for perpendicular magnetic recording media," *IEEE Trans. Magn.*, vol. 24, no. 6, pp. 3024–3026, 1988.
- [19] X. Liu, J. Bai, F. Wei, Z. Yang, A. Morisako, and M. Matsumoto, "Barium ferrite thin films prepared by alternate deposition," *J. Magn. Magn. Mater.*, vol. 212, no. 1, pp. 273–276, 2000.
- [20] X. Liu *et al.*, "Magnetic and crystallographic properties of La–Zn substituted Sr-ferrite thin films," *J. Appl. Phys.*, vol. 87, no. 9, p. 6875, 2000.
- [21] J. Feng, N. Funabashi, N. Matsushita, S. Nakagawa, and M. Naoe, "Increase of coercivity and squareness ratio of Ba ferrite thin films by adding SiO₂ and substituting Al for Fe," *IEEE Trans. Magn.*, vol. 36, no. 5 I, pp. 2930–2932, 2000.
- [22] M. E. Koleva *et al.*, "Sr-ferrite thin films grown on sapphire by pulsed laser deposition," *Appl. Surf. Sci.*, vol. 168, no. 1–4, pp. 108–113, 2000.
- [23] S. Nakagawa, N. Matsushita, and M. Naoe, "Perpendicular magnetic recording media using hexagonal ferrite thin films deposited on Pt underlayers and interlayers," *J. Magn. Magn. Mater.*, vol. 235, no. 1–3, pp. 337–341, 2001.
- [24] S. Capraro *et al.*, "Properties of barium ferrite sputtered films," *Sensors and Actuators A-Physical*, vol. 113, no. 3, pp. 382–386, 2004.
- [25] S. Capraro *et al.*, "Crystallographic properties of magnetron sputtered barium ferrite films," *Mater. Sci. Eng. B Solid-State Mater. Adv. Technol.*, vol. 112, no. 1, pp. 19–24, 2004.
- [26] S. Anjum *et al.*, "Investigation of induced parallel magnetic anisotropy at low deposition temperature in Ba-hexaferrites thin films," *J. Magn. Magn. Mater.*, vol. 324, no. 5, pp. 711–716, 2012.
- [27] H. Xu, W. Zhang, B. Peng, and W. Zhang, "Properties of barium hexa-ferrite thin films dependent on sputtering pressure," *Appl. Surf. Sci.*, vol. 257, no. 7, pp. 2689–2693, 2011.
- [28] W. Zhang, B. Peng, W. Zhang, S. Zhou, and H. Schmidt, "Ultra large coercivity in barium ferrite thin films prepared by magnetron sputtering," *J. Magn. Magn. Mater.*, vol. 322,

no. 13, pp. 1859–1862, 2010.

- [29] H. Hassane, J. P. Chatelon, J. J. Rousseau, A. Siblini, and A. Kriga, “Influence of Magnetron Effect on Barium Hexaferrite Thin Layers,” *Adv. Mater. Res.*, vol. 324, pp. 97–100, 2011.
- [30] S. M. Masoudpanah, S. A. S. Ebrahimi, and C. K. Ong, “Magnetic properties of strontium hexaferrite films prepared by pulsed laser deposition,” *J. Magn. Magn. Mater.*, vol. 324, no. 17, pp. 2654–2658, 2012.
- [31] S. M. Masoudpanah and S. A. Seyyed Ebrahimi, “Influence of metal precursor on the synthesis and magnetic properties of nanocrystalline SrFe₁₂O₁₉ thin films,” *J. Magn. Magn. Mater.*, vol. 343, pp. 276–280, 2013.
- [32] M. Khaleeq-ur-Rahman, K. A. Bhatti, M. S. Rafique, and A. Latif, “Deposition and characterization of strontium hexa ferrite (SrFe₁₂O₁₉) by PLD technique,” *Opt. Laser Technol.*, vol. 47, pp. 361–365, 2013.
- [33] S. M. Masoudpanah and C. K. Ong, “SrFeO amorphous underlayer for fabrication of c-axis perpendicularly orientated strontium hexaferrite films by pulsed laser deposition,” *J. Magn. Magn. Mater.*, vol. 341, pp. 36–39, 2013.
- [34] T. Garcia *et al.*, “Polycrystalline SrFe₁₂O₁₉ thin films grown by pulsed laser deposition,” in *3rd Iberoamerican Optics Meeting and 6th Latin American Meeting on Optics, Lasers, and Their Applications*, 1999, pp. 78–83.
- [35] K. Sun *et al.*, “Magnetic property and stress study of barium hexaferrite thin films with different structures,” *J. Alloys Compd.*, vol. 663, pp. 645–650, 2016.
- [36] Y. Hoshi, Y. Kubota, and M. Naoe, “Control of orientation and crystallite size of barium ferrite thin films in sputter deposition,” *IEEE Trans. Magn.*, vol. 31, no. 6 pt 1, pp. 2782–2784, 1995.
- [37] Y. Hoshi, Y. Kubota, and H. Ikawa, “Preparation of c-axis-oriented barium ferrite thin films with small crystallite size,” *J. Appl. Phys.*, vol. 81, no. 8, p. 4677, 1997.
- [38] E. Lacroix, P. Gerard, D. Challeton, B. Rolland, and B. Bechevet, “ELABORATION OF M-TYPE Ba-FERRITES FILMS BY R.F. SPUTTERING,” 1988.
- [39] A. Morisako, M. Saitoh, and M. Matsumoto, “Magnetic properties of sputtered strontium ferrite films prepared from sintered target with Fe/Sr composition ratio of 8–14,” *J. Appl. Phys.*, vol. 85, no. 8, p. 4732, 1999.
- [40] T. S. Cho, S. J. Doh, J. H. Je, and D. Y. Noh, “Thickness dependence of the crystallization of Ba-ferrite films,” *J. Appl. Phys.*, vol. 86, no. 4, pp. 1958–1964, 1999.
- [41] A. Morisako, M. Saitoh, M. Matsumoto, A. Morisako, M. Saitoh, and M. Matsumoto, “Effect of chromium addition on the properties of sputtered strontium ferrite films Effect of chromium addition on the properties of sputtered strontium ferrite films,” vol. 6872, no. 2000, pp. 1998–2001, 2003.

- [42] P. Hing, J. M. Ray, C. S. Fong, O. J. Tien, and W. Jianfeng, "Sputtering effects on magnetic properties of BaM thin film," *J. Mater. Sci. Lett.*, vol. 21, no. 10, pp. 823–826, 2002.
- [43] B. Bayard, J. P. Chatelon, M. Le Berre, H. Joisten, J. J. Rousseau, and Barbier, "The effects of deposition and annealing conditions on crystallographic properties of sputtered barium ferrite thick films," *Sensors Actuators, A Phys.*, vol. 99, no. 1–2, pp. 207–212, 2002.
- [44] S. Capraro *et al.*, "Magnetic properties of sputtered barium ferrite thick films," *J. Appl. Phys.*, vol. 93, no. 12, pp. 9898–9901, 2003.
- [45] A. R. Abuzir and W. J. Yeh, "Comparison Between In-situ Annealing and External Annealing For Barium Ferrite Thin Films Made by RF Magnetron Sputtering," vol. 875, pp. 1–6, 2005.
- [46] X. Zhang, Z. Yue, and L. Li, "Orientation Growth and Magnetic Properties of BaM Hexaferrite Films Deposited by Direct Current Magnetron Sputtering," *J. Am. Ceram. Soc.*, vol. 99, no. 3, pp. 860–865, 2016.
- [47] S. Verma, O. P. Pandey, A. Paesano, and P. Sharma, "Comparison of structural and magnetic properties of La₃ + substituted BaFe₁₂O₁₉ prepared by different substitution methods," *Phys. B Condens. Matter*, vol. 448, pp. 57–59, 2014.